

### Science Forum (Journal of Pure and Applied Sciences)



# Morphology and geochemical signatures of diatexite migmattes around Mararaban Liman Katagum, Bauchi State, North Eastern Nigeria



Danjuma Daure<sup>1\*</sup>, Ahmed Isah Haruna<sup>1</sup>, Saidu Abdullahi<sup>2</sup>, Lasisi Oladimeji Yusuf<sup>1</sup>

- <sup>1</sup> Department of Applied Geology, Abubakar Tafawa Balewa University, Bauchi, Nigeria
- <sup>2</sup> Department of Geological Sciences, Federal University, Gusau, Nigeria

#### **ABSTRACT**

The Migmatites of the study area fall under the older granite that constitutes the Basement complex of Nigeria. The aim of this research is to present the result of a geochemical investigation of Migmatites in the study area. Diatexite migmatites, which include melanocratic, mesocratic, and leucocratic diatexites covered almost all of the study area, around Mararaban Liman Katagum, Bauchi, in North-eastern Nigeria. Geochemically, these rocks show high SiO, in the range of 65.81-83.12wt% with an average of 74.43wt%, Al2O, and FeO, enrichment are pronounced in the rock samples ranging from 10.02 to 13.80 and 1.06 to 11.21 showing an average of 12.59wt% and 11.05wt%, respectively. In addition, Na<sub>2</sub>O remains consistently less than K<sub>2</sub>O in the range of 0.06-1.84 and 0.6-6.4 respectively in most of the samples. The rocks are generally depleted in CaO, SO<sub>2</sub>, MgO, P<sub>2</sub>O<sub>5</sub>, and MnO in the range of 0.02-0.82, 0.005-1.23, 0.01-3.84, 0.006-0.16, and 0.004-0.21, respectively. They are peraluminous with S-type characteristics, magnesian to ferroan. The diatexite migmatites show a clear arc-like signature as seen in the depletion in high field strength elements (HFSE) and enrichment in large ion lithophile elements (LILE), and LILE enhancement relative to HFSE signifies subduction-zone enrichment and/or crustal mixing of the source region.

#### **ARTICLE INFO**

Artcle history:

Received 21 January 2023 Received in revised form 30 May 2023 Accepted 01 June 2023 Published 15 January 2024 Available online 15 January 2024

#### **KEYWORDS**

Migmatite Melanocratic Mesocratic Leucocratic

#### 1. Introduction

Migmatites have been recognized across most of the geological time, develop in various tectonic settings, and can affect a wide range of protoliths (Sawyer, 2008).

The Migmatites of the study area fall under one of the three major lithological units that constitute the Basement complex of Nigeria.

The study area which occurs within the Precambrian basement complex of north-eastern Nigeria is located around Mararaban Liman Katagum within Latitudes N10° 06′ 04.0″, N10° 05′ 13.4″, and Longitude E009° 41′ 05.2″, E009° 39′ 49.2″, and covers an area of about 25 km² (Fig. 1). The area has appreciable relief typified by high- and low-level outcrops, and most of the high-level outcrops and hills characterized by conically shaped outlines have a height ranging from 620 to 635 m above mean sea level as depicted in the physiographic map (Fig. 2).

This study examines the geochemical variations that occur during the anatexis of siliciclastic metased-imentary rocks, where a relatively large volume of granitic magma developed from diatexite migmatites.

<sup>\*</sup> Corresponding author Danjuma Daure ☑ danjtal@gmail.com ☑ Department of Applied Geology, Abubakar Tafawa Balewa University, Bauchi, Nigeria.

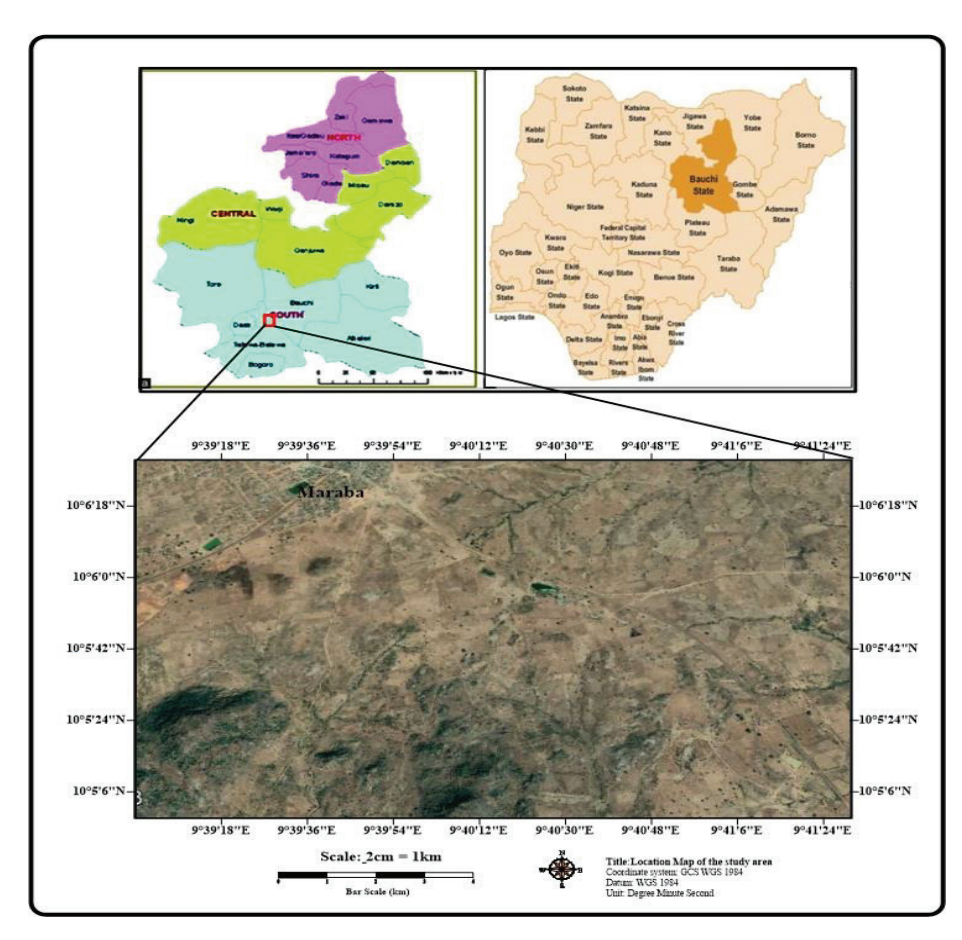


Figure 1. Location map of the study area (Source: Google earth).

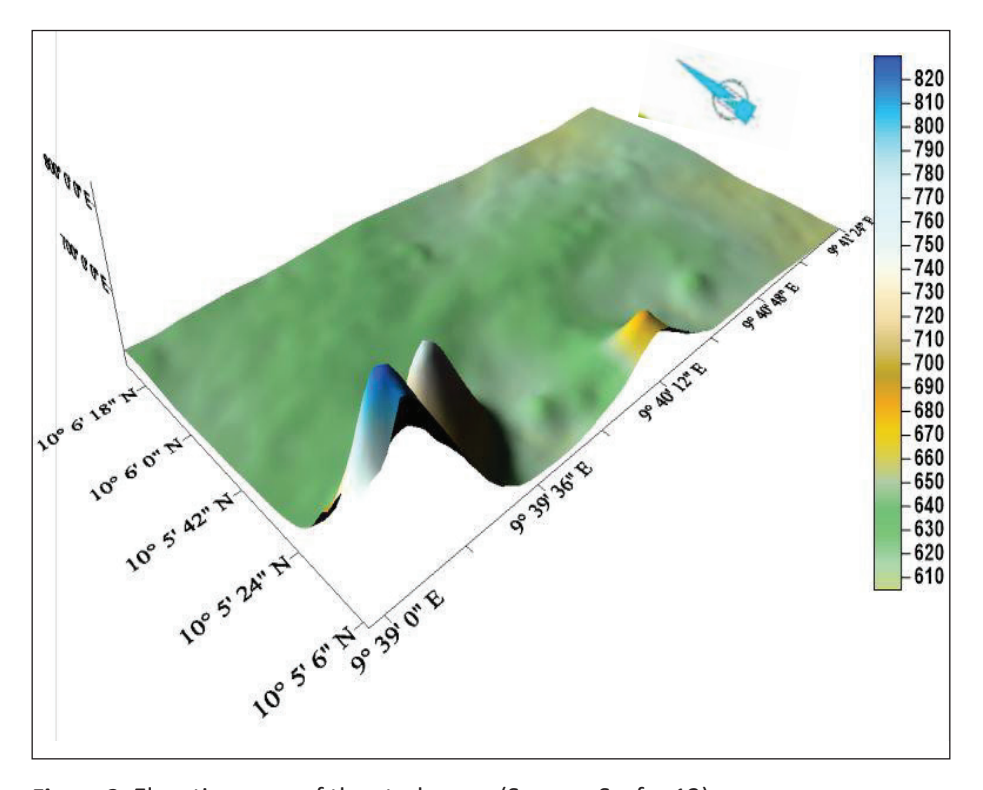


Figure 2. Elevation map of the study area (Source: Surfer 12).

#### 2. Geological Settings

The Precambrian Basement Complex of Nigeria lies within the Pan-African mobile belt, east of the West African craton and northwest of the Congo-Gabon craton (Black et al., 1979; Burke et al., 1972; Caby et al., 1981; Leblanc, 1981).

The collision at this plate margin is believed to have led to the reactivation of the internal region of the Pan-African belt. The Nigerian Basement Complex lies within the reactivated part of the belt (Rahaman, 1991).

The study area (Fig. 4) falls within the region dominated by crystalline rocks including gneisses, migmatites, and metasediments of Precambrian age. The major rock units of the area include granite gneiss, migmatitic gneiss, and diorite. Others include granites and pegmatites (Haruna et al., 2008).

#### 3. Material and Method

The fieldwork started with a reconnaissance survey of the area especially the access roads, drainage channels, and types of settlements, and also taking note of the minor and major outcrops. This was followed by detailed geological mapping (Fig. 3) involving the traverse method of field mapping, collection of representative rock samples from outcrops, road cuts, etc.

Strikes and dips of outcrops and structures were taken with compass clinometers, and their location was recorded with the global positioning system.

Fourteen samples out of 25 were selected for the geochemical analyses and were air-dried at room temperature, after which they were crushed in a Laboratory Jaw Crusher. The resultant samples were pulverized in a Vibrating Disc Mill. Final size reduction, mixing, and homogenization to <75 pm were done with a Mixer Mill. About 8.0 g each of the 14 samples were, thereafter, taken to Nigeria Geological Survey Agency Analytical Laboratories, Kaduna, Nigeria, for major and trace element geochemistry using inductively coupled mass spectrophotometer and X-ray fluorescence techniques. The geochemical data for petrology were interpreted with Geochemical Data Toolkit and Petrograph software through the use of various discrimination diagrams. Descriptive statistics and multivariate statistics were used to establish the distribution, interelement, and intersample variability.

#### 4. Results and Discussion

Migmatites can be divided into two first-order groups; metatexites and diatexites. Metatexites are migmatites

that preserve coherent, pre-partial melting structures in the palaeosome and residuum, whereas diatexites have disaggregated and lost structural coherency Sawyer (2008). The study area falls under the diatexite classification of migmatite which is variable in appearance as it typically includes leucocratic, mesocratic, and melanocratic in varying proportions as described in the following section

## **4.1.** Field relationship and macroscopic descriptions of the rocks

Melanocratic diatexite has the highest biotite contents of the other diatexite types in the study area. They are generally well-foliated (Plate 1a and b) rocks (containing oriented biotite and plagioclase) and many are also flow banded on a centimeter scale; rich in quartz, plagioclase, K-feldspar, and apatite.

Mesocratic diatexite of the study area is generally medium to coarse grain size and a relatively uniform texture with locally elongate euhedral plagioclase defining a magmatic foliation (Plate 2a) shows mesocratic diatexite with schlieren characterized by well-developed, flow-induced structures, defined by thin layers of aligned platey, tabular, or prismatic minerals.

Leucocratic diatexite of the study area are generally coarse-grained and local domains have a well-defined igneous texture (with crystal faces developed on feldspar against quartz) and, local flow-oriented plagioclase and K-feldspar phenocrysts. Schollen diatexite migmatite (Plate 3a) commonly occurs at the transition from metatexite to diatexite and represents the disaggregation of the palaeosome, melanosome, and resister lithologies into discrete blocks thereby disrupting the structural continuity.

#### 4.2. Geochemical composition

Major and trace elements distributions of the diatexite migmatite of the area are represented in Table 1. Major element concentrations in the studied rocks fully reflect their granitic character. The major elements composition shows that the rocks are characterized by high SiO<sub>2</sub> in the range of 65.81-83.12 wt% with an average of 74.43wt%, Al2O<sub>3</sub> and FeO<sub>3</sub> enrichment are pronounced in the rock samples ranging from 10.02 to 13.80 and 1.06 to 11.21 showing an average of 12.59wt% and 11.05wt%, respectively. In addition, Na<sub>2</sub>O remains consistently less than K<sub>2</sub>O in the range of 0.06 to 1.84 and 0.6 to 6.4 respectively in most of the samples. The rocks are generally depleted in CaO,  $SO_2$ , MgO,  $P_2O_5$ , and MnO in the range of 0.02-0.82, 0.005-1.23, 0.01-3.84, 0.006-0.16, and 0.004-0.21, respectively.

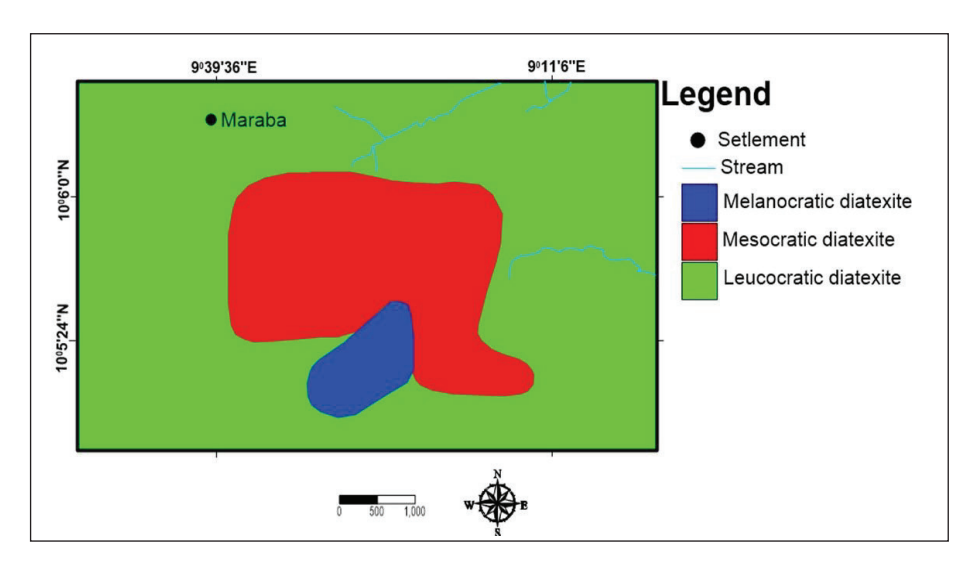
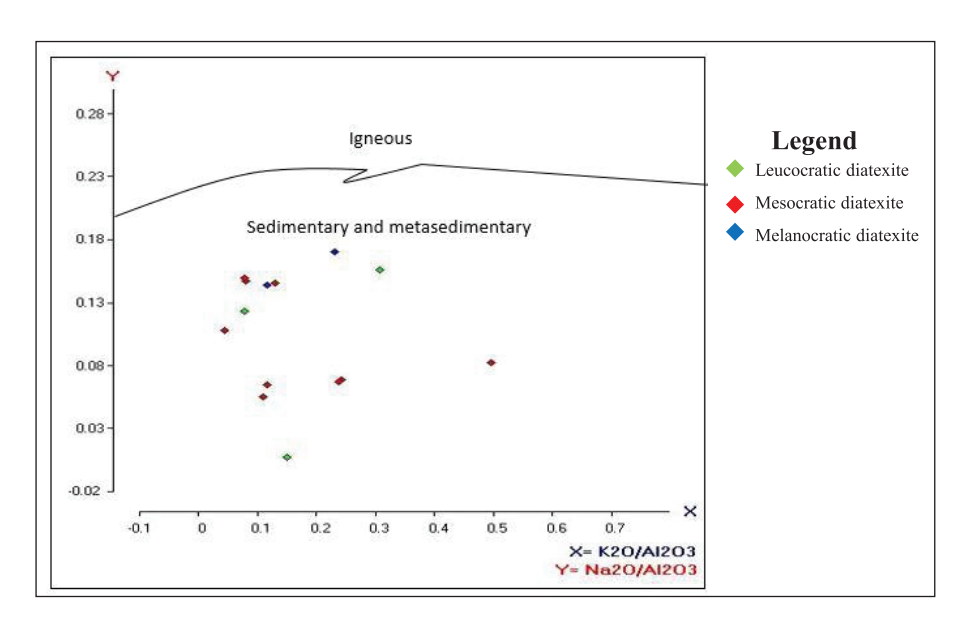
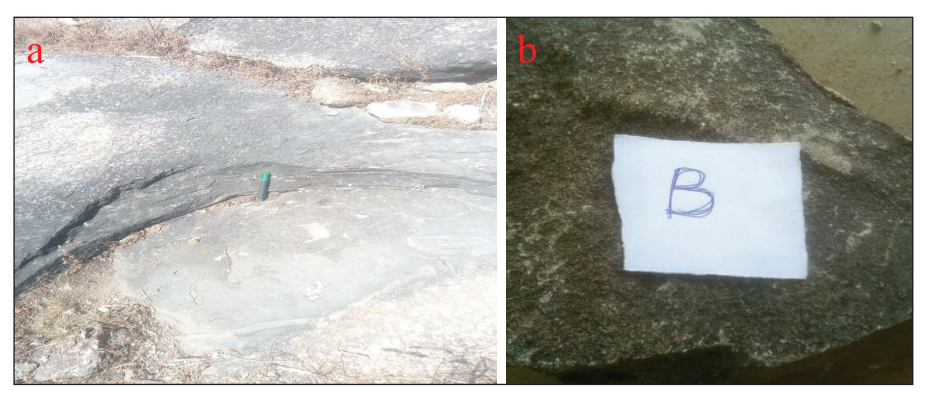


Figure 3. Geological map of the study area.



**Figure 4.** Na<sub>2</sub>O/Al<sub>2</sub>O<sub>3</sub> versus K<sub>2</sub>O/Al<sub>2</sub>O<sub>3</sub> plot (after Garrells and Mackenzie, 1971).



**Plate 1.** (a) Field occurrence of melanocratic diatexite of the study area (b) hand sample appearance of melanocratic diatexite migmatite.

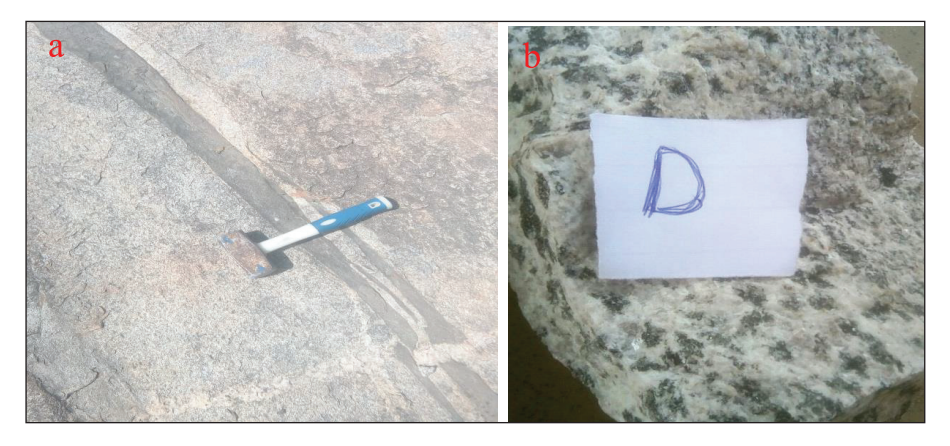


**Plate 2.** (a) Field occurrence of mesocratic diatexite of the study area containing schleiren (b) hand sample appearance of mesocratic diatexite migmatite.



**Plate 3.** (a) Field occurrence of leucocratic diatexite of the study area (b) hand sample appearance of leucocratic diatexite migmatite.

#### 4.3. Provenance

The protoliths could have been derived from the partial melting of metasedimentary rocks. The sedimentary nature of these rocks is supported by their position in the diagram such as  $Na_2O/Al_2O_3$  vs.  $K_2O/Al_2O_3$  (after Garrells and Mackenzie, 1971) as shown in Figure 4.

#### 4.4. Harker variation diagram

In the diatexite migmatite rocks, CaO, MgO,  $Al_2O_3$ , and  $Fe_2O_3$  display a negative correlation with  $SiO_2$  in the Harker plot suggesting fractional crystallization.  $K_2O$  is fairly positively correlated with  $SiO_2$  (Fig. 5).

#### 4.5. Tectonic discrimination

According to the classification of granitoid rocks by Frost et al. (2001) in Figure 6, the diatexite belongs to the ferroan group (only 3 samples of diatexite migmatite belong to the magnesian group). In the modified alkali lime index, MALI of Frost et al. (2001) the diatexite migmatite plot across two different trends of calc-alkalic and calcic series suggesting multiple

magma crystallization processes. The strongly peraluminous, fairly potassic, and high silica content of the rocks clearly further supports the inference that the diatexite migmatite of the area metamorphosed from sedimentary and/or metasedimentary protoliths.

#### 4.6. Feldspar diagram

When projected in the feldspar diagram (Fig. 7), the samples define a trend away from the Ca field toward the Na apex, reflecting their low Ca content. On the other hand (Fig. 7b), the samples define a trend across the alkali feldspar field. In Figure 7a, melanocratic diatexite is enriched in Na compared to mesocratic and leucocratic diatexites. Within the alkali feldspar group, the leucocratic diatexite is richer in K than the melanocratic and mesocratic diatexites (Fig. 7b). This is related to Bowen reaction series (Fig. 8) and suggests upper-amphibolite facies metamorphism occurred in the area.

#### 4.7. Spider diagram

In the incompatible trace-element concentrations normalized by Chondrite, after Thompson (1982)

**Table 1.** Major and trace element composition of diatexite migmatite of the study area.

Oxides Composi tion %	Melanocratic diatexite		Mesocratic diatexite										Leucocratic diatexite		
	S 11A	S not	S 17	S 23	S 14B	S 3	S 1	S 7	S 8	S 24	S 11C	S 18A	S 9	S 14	
SiO <sub>2</sub>	65.81	68.12	73	73	73.5	73.66	74.08	74.31	74.76	75.1	75.3	77.89	80.38	83.12	
CaO	0.13	0.11	0.2	0.03	0.67	0.6	0.7	0.42	0.82	0.02	0.3	0.6	0.32	0.21	
MgO	3.84	2.84	0.1	0.01	2	0.29	0-31	0.15	0.21	ND	0.05	0.08	0.08	0.02	
SO <sub>3</sub>	1.2	1.23	ND	0.01	0.15	0.02	0.01	0.005	0.007	ND	ND	0.23	ND	0.03	
$K_2^0$	2.51	1.5	1.8	1.11	0.6	3.21	1.6	6.4	3.24	1.45	1.06	3.08	1.8	0.83	
Na <sub>2</sub> O	1.84	1.84	2	2	1.41	0.9	0.88	1.06	0.9	0.72	2	1.56	0.08	1.28	
TiO <sub>2</sub>	1.13	1.14	0.5	2.3	0.45	0.51	0.42	0.1	0.4	0.22	0.76	2	1	0.84	
MnO	0.11	0.21	0.02	0.2	0.13	0.03	0.02	0.01	0.02	0.004	0.14	0.04	0.004	0.19	
$P_2O_5$	0.01	0.02	ND	0.03	0.16	ND	ND	0.006	ND	ND	ND	ND	ND	ND	
Fe <sub>2</sub> O <sub>3</sub>	11.21	9.2	6.01	8.48	4.8	5.01	4	3.02	4.21	1.06	3.76	10.18	3.89	8.07	
$Al_2O_3$	10.82	12.83	13.8	13.6	13.1	13.2	13.6	12.89	13.53	13.1	13.4	10.02	12	10.4	
H <sub>2</sub> O <sup>+</sup>	3	2.01	1.6	2.12	1.81	2.5	2.03	1.62	1.9	2.1	2.46	1.5	1.07	1.6	
Trace element(ppm)															
V	401.01	431	412	640	515	623	511.5	725	722	442	326	631	335	427	
Cr	118.02	135.29	243	326	233.19	315	256.19	219.02	232	241	145.5	246.29	102.1	214.4	
Cu	480	334	330	380	310	290	354	425	415	334	312	330	163	286	
Sr	1,894	1,620	2,060	1,833	1,240	280	1,320	2,240	2,200	2,011	2,032	1,250	1,225	1,070	
Zr	5,710	1,240	1,520	1,205	1,030	720	1,205	1,650	1610	1,530	1,510	1,220	701	1,040	
Ва	670	3,110	1,820	2,110	960	100	3,100	690	692	1,810	1,820	2,100	920.88	660	
Zn	100	97	560	370	40	61	97	58.5	68	57	550	127	20.5	167	
Ce	33	51	4	23	41	45	50.5	58	57	54	53	55	64	80.65	
Pb	75.5	26.5	847.5	66.09	25.5	17.5	26.5	83	84.6	857	864	36	72.05	584	
Bi	0.244	0.099	0.871	5	1.89	0.219	0.099	0.451	0.45	0.873	0.673	0.099	1	3.58	
Ga	34.02	39.5	22	5.09	32	17.4	39	26	26.5	42	12.5	37	32.6	6.5	
As	22	7.02	17.2	3.5	15	6	7.02	15.05	15.15	17.3	16	7.12	25	0.4	
Υ	9	15.5	3.5	4.35	14	39.1	14	2.9	2.93	3.92	3.6	15.2	21	26.5	
lr	5.1	20	6.09	4.02	3.15	3.1	20.5	2.06	5.06	6.07	6	30	28.5	3	
Au	1.67	0.32	0.448	0.2	0.424	0.014	0.22	0.53	0.43	1.468	0.485	0.42	0.84	1.6	
Ni	0.046	<0.001	<0.001	<0.001	0.038	<0.001	<0.001		<0.001		<0.001	<0.001	<0.001	<0.001	
Rb	22.6	29.8	33.4	36.5	30	9.84	29	39.03	39	30	30.5	29.5	23	69	
Mo	15.5	32	83.5	0.01	48.5	14.07	32	<0.001	<0.001	81.05	83.05	0.51	<0.001	0.008	
Co	0.001	0.001	0.213	<0.001	0.04	0.01	<0.001	5.5	5	0.24	0.212	<0.001	1.03	0.998	
Cd	0.06	0.03	1.192	0.005	0.998	<0.001	0.034	<0.001	<0.001	1.094	1.093	0.534	0.002	<0.001	
Ru	0.035	0.015	0.005	1.22	0.002	<0.001	0.005	8.6	8.65	0.001	<0.001	0.006	5	0.78	
Eu	1.65	0.25	2.06	340	1.24	0.82	0.14	38.5	38	2.06	2	0.22	51	23.5	
Re	160.5	185.5	36.02	<0.001	120	101	170	<0.001	<0.001	36	35	10.3	0.106	0.004	
Nb	18.22	17.52	20.3	42.5	20.12	14.35	30.22	18	16	25	43.87	40.3	10.15	60.5	
Ag	0.6	0.41	0.09	0.54	1.12	0.67	0.11	1.2	1.2	0.09	0.007	0.4	0.8	1.1	
Та	70.2	42,10	64.2	55	36	63	42.10	41.5	41.2	61	68	42.5	34	101.5	
W	12	0.891	1.46	5.06	0.96	13.3	0.891	0.882	0.882	1.46	1.76	0.801	7.54	5.6	
Hf	39.45	33	21	24	20	16	33	11	11	21	21.5	33.5	16.62	25	
Yb	2.14	4.04	6.9	0.46	2.11	1.76	4.14	5.9	5.9	6.9	6.66	2.04	1.04	0.19	

Continued

Oxides Composi tion %	Melanocratic diatexite		Mesocratic diatexite										Leucocratic diatexite		
	S 11A	S not	S 17	S 23	S 14B	S 3	S 1	S 7	S 8	S 24	S 11C	S 18A	S 9	S 14	
In	9.72	2.1	0.09	2.23	1.9	3	2.1	8	8	0.09	0.07	4.1	4.5	2.3	
Se	0.2	< 0.001	0.012	0.28	0.21	0.28	< 0.001	<0.001	< 0.001	0.012	0.03	0.001	0.4	0.42	
U	0.201	< 0.001	0.007	< 0.001	0.022	< 0.001	0.001	<0.001	< 0.001	0.007	0.001	< 0.001	0.101	0.025	
Th	0.31	2.5	2.2	0.31	0.86	0.22	1.5	0.2	0.25	2.2	0.2	1.5	0.14	0.08	
Sb	8.01	7.03	14	3.3	6.13	12	7.03	3.24	3.34	14	10	7.5	0.55	2.2	
Ge	24.01	20	41	4.36	4.6	14	24	68	68.5	40	45	22	36.41	18.85	
Sn	1.22	31.56	19.12	19.88	17.03	9.88	21.06	43.4	45.4	21.12	27.02	31.25	50.55	45.43	

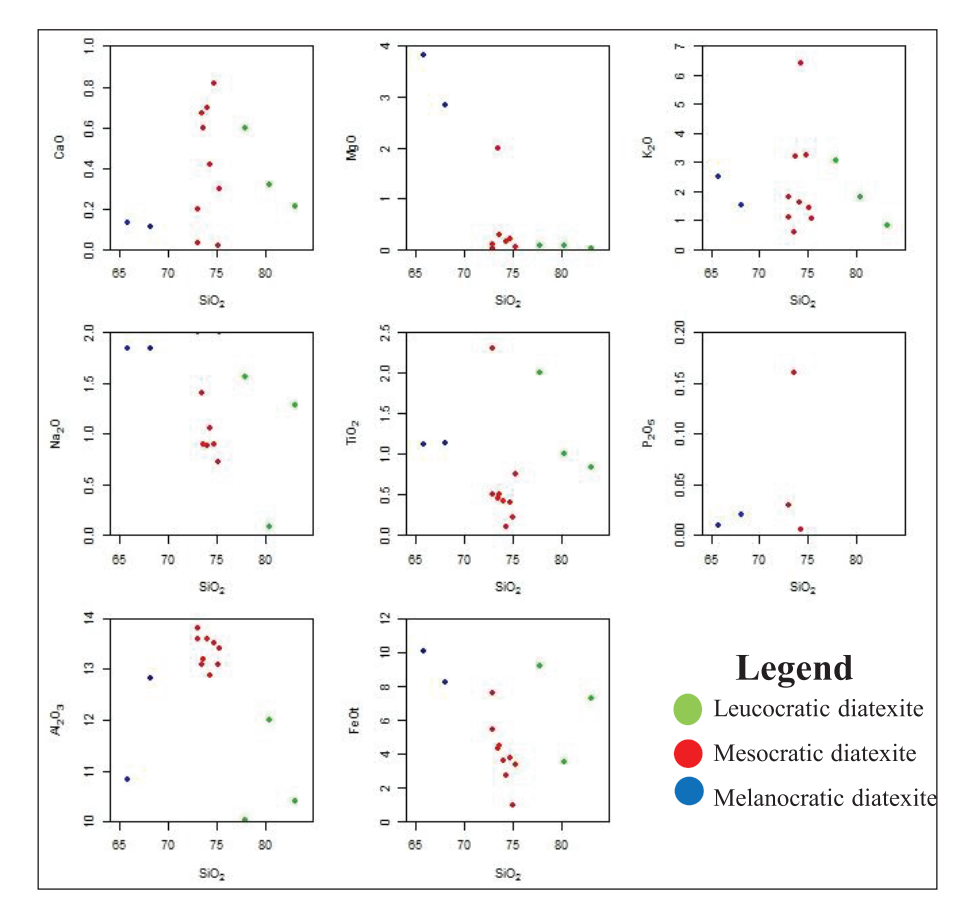


Figure 5. Harker diagrams of major elements for the diatexite migmatite.

(Fig. 9), the diatexite migmatites display a near negative linear trend characterized by decreasing abundance from large ion lithophile elements down to high field strength elements. The migmatites display a gentle slope with positive Ba, Rb, Th, K, Nb, Ta, Ce, Sr, Zr, and Hf, and, there is depletion in Th, Ce, and Sr. The diatexite migmatites show enrichment in Ba, Rb,

K, Ta, Sr, Zr, Hf, and negative P, Ti, and Yb anomalies. Fractional crystallization is reflected in the differences in the samples which indicate melts formed by mixing of mafic melt with crustal components during ascent, and thus, the diatexite migmatite follows sub-parallel alkali-lime trends during differentiation (Frost et al., 2001).

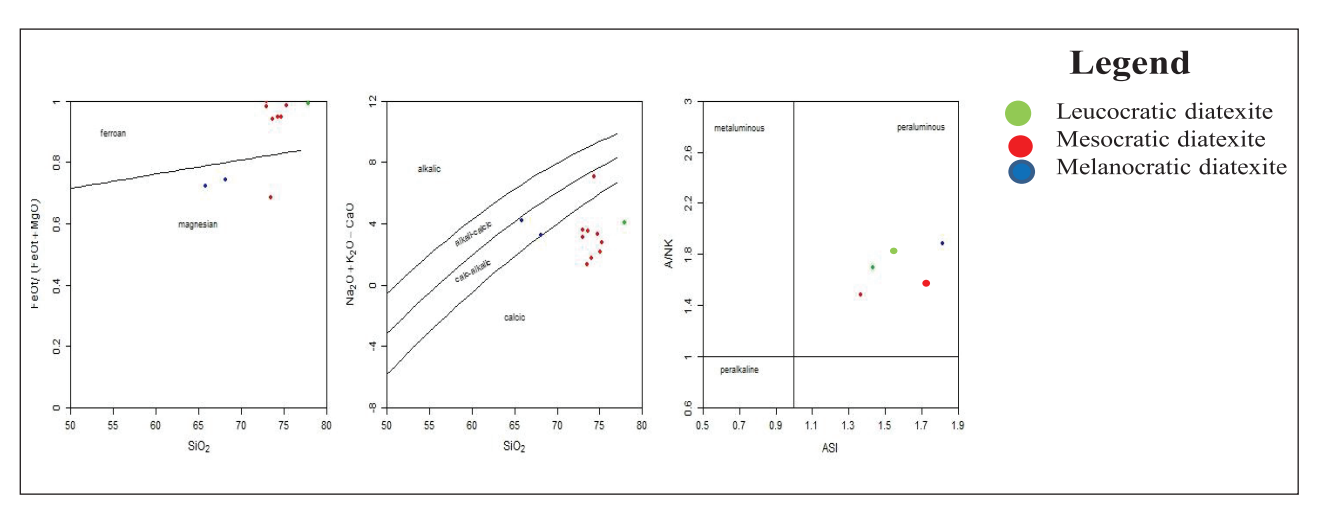


Figure 6. Plot of tectonic discrimination, (Frost et al., 2001).

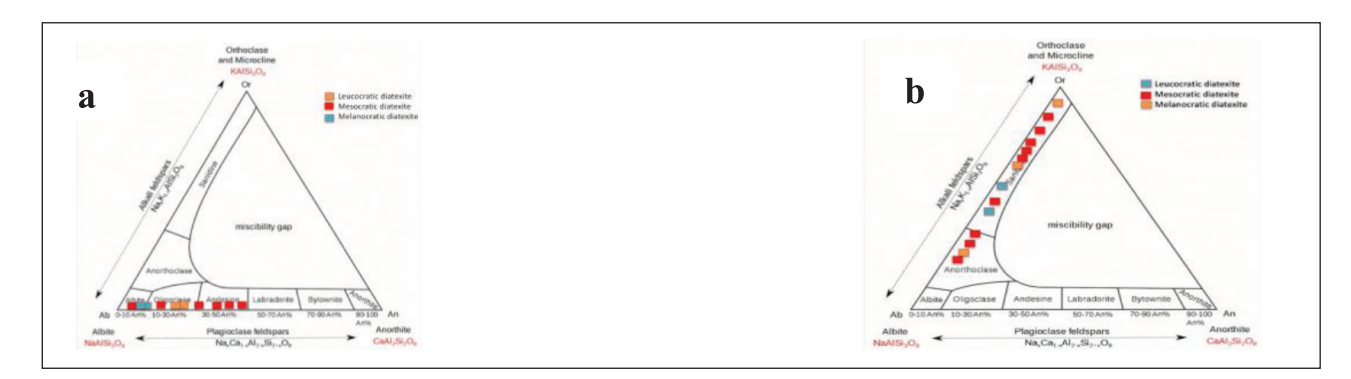


Figure 7. (a and b): Feldspar diagram.

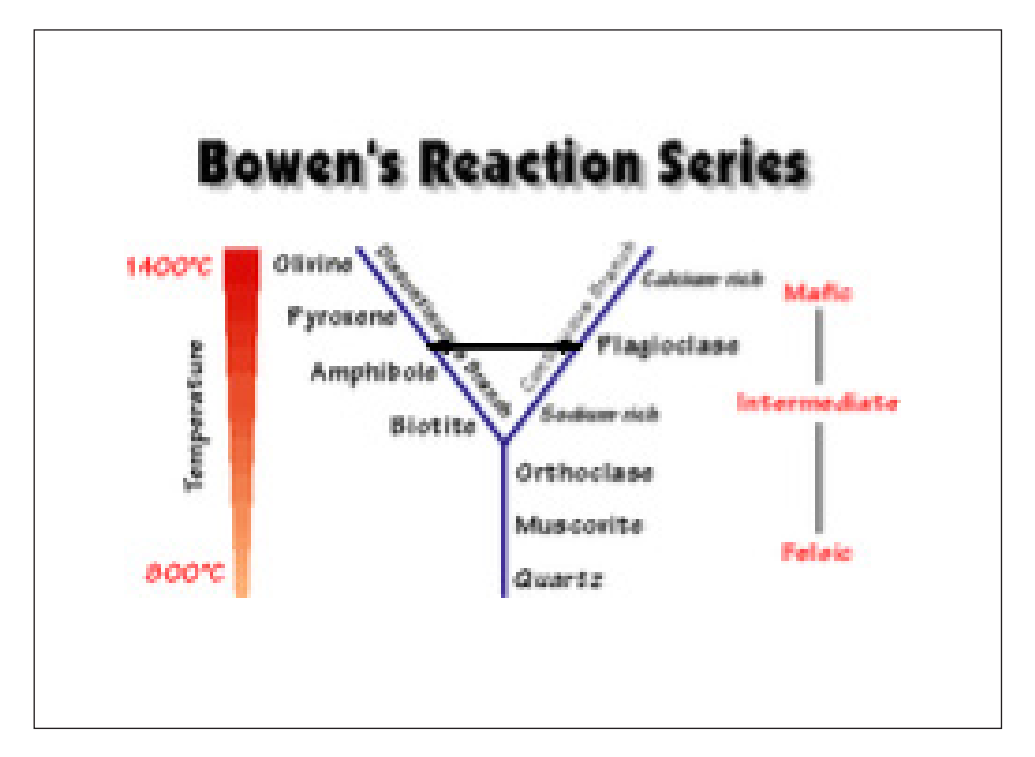
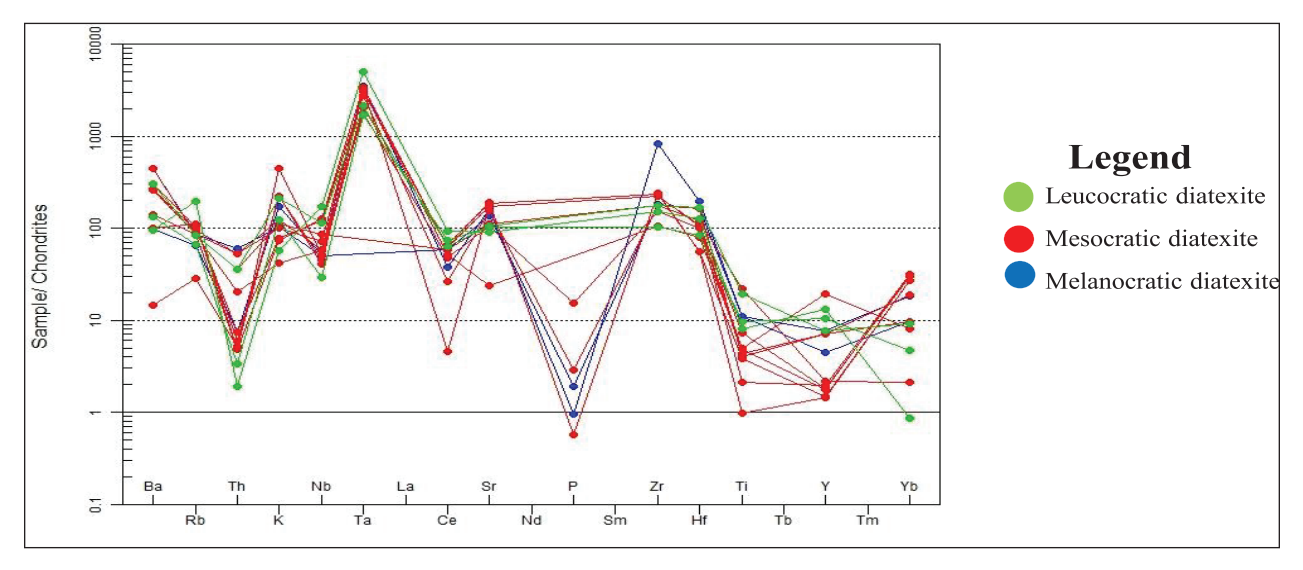


Figure 8. Bowen continuous and discontinuous reaction.



**Figure 9.** Chondrite-normalized incompatible element patterns for diatexite mimatite normalization values from Thompson (1982).

#### 5. Conclusion

The study area consists of migmatites with morphological and geochemical continuity within the different identified groups (melanocratic, mesocratic, and leucocratic diatexites). Diatexite migmatites of the study area constitute the basement rocks. The diatexite migmatites are thought to have evolved from both partial melting and metamorphic crystallization. A sedimentary and/or metasedimentary protolith has been interpreted for the metamorphosed rocks in the area which are largely peraluminous. The variations in the lithologic units within the area may have been due to differences in the compositions of the sedimentary progenitors.

#### 6. Recommendations

Having studied the diatexite migmatites around Mararaban Liman Katagum, Bauchi State, the following recommendations may be useful:

- i. Enriching researchers with tools to further investigate processes and mineralization potentials of the rocks;
- ii. Studies involving structural analyses of the study area are recommended;
- iii. Establishment of the quarry so as to create job opportunities;
- iv. Enriching researchers with tools to further conduct isotope study of the rocks in order to come up with conclusive findings; and
- v. Fluid inclusion studies are also recommended to provide direct information about the conditions under which the rocks were formed.

#### **Acknowledgment**

The authors would like to thank the Department of Applied Geology, Abubakar Tafawa Balewa University, Bauchi, for providing the equipment used in this research and to Nigerian Geological Survey Agency (NGSA), Kaduna, for the geochemical analyses of the samples as well as individuals like Yusuf Baba, etc for their financial supports.

#### References

Black R, Caby R, Moussine-Pouchkine A, Bayer R, Betrand JM, Boullier MM, et al. Evidence for late Precambrian plate tectonics in West Africa. Nature 1979; 278(5701):223-7.

Burke KC, Freeth SJ, Grant IK. Granite gneiss in the Ibadan area, Nigeria. African geology. Geology Department, University of Ibadan, Ibadan, Nigeria, pp 103–4, 1972.

Caby R, Betrand JML, Black R. Pan-African ocean closure and continental collision in the Hogger-Iforas segment, central sahara. In: Kroner A (ed.). Precambrian plate tectonics, Elsevier, Amsterdam, The Netherlands, pp 407–37, 1981.

Garrels RM, Mackenzie FT. Gregor's denudation of the continents. Nature 1971; 231(5302):382–3.

Haruna IV, Dada SS, Mamman YD. Stream sediment geochemical survey of an area around Dass, NE Nigeria. Glob J Geol Sci 2008; 6(2):105–12.

Frost BR, Barnes CG, Collins WJ, Arculus RJ, Ellis DJ, Frost CD. A geochemical classification for granitic rocks. J Petrol 2001; 42(11):2033–48.

Frost BR, Lindsley DH. Occurrence of irontitanium oxides in igneous rocks. In: Lindsley DH (ed.). Reviews in

- mineralogy and geochemistry. DE Gruyter, Berlin, Germany, Vol. 25, pp 433–68, 1991.
- Leblanc M. The late Proterozoic ophiolites of Bou Azzer (Morocco): evidence for Pan-African plate tectonics. In: Kroner A (Ed.). Precambrian plate tectonics, Elsevier, Amsterdam, Netherlands, pp 435–51, 1981.
- Rahaman MA, Tubosun IA, Lancelot JR. U-Pb geochronology of potassic syenites from Southwestern Nigeria and
- the timing of deformational events during the Pan-African orogeny. J Afr Earth Sci 1991; 13(3–4):387–95.
- Sawyer EW. Working with migmatites. Mineralogical association of Canada short course series. Mineralogical Association of Canada, Quebec City, Canada, Vol. 38, p 1–28, 2008.
- Thompson RN. Magmatism of the British tertiary volcanic province. Scott J Geol 1982; 18(1):49–107.